Collision Induced Dissociation of Deprotonated Glycolaldehyde

In the formose or Butlerov reaction, formaldehyde oligomerizes to form carbohydrates and this reaction is considered to be the source of prebiotic sugar formation on early Earth [Butlerow, 1861]. The first step of this reaction involves the formation of glycolaldehyde from two formaldehyde molecules.

$$2\,HCHO \longrightarrow CH_2OHCHO \tag{5.1}$$

$$HCHO + HCO^- \longrightarrow {}^-CH_2OCHO \tag{5.2}$$

In solution, this reaction has been proposed to occur between a deprotonated formaldehyde (HCO^- anion formed under basic conditions) and a neutral formaldehyde molecule [Breslow, 1959]. Studies have shown that the proposed mechanism was not entirely correct and further experimental and computational investigations of the formose reaction have been reported [Ricardo *et al.*, 2006; Appayee and Breslow, 2014; Jalbout *et al.*, 2007; Wang and Bowie, 2010; Halfen *et al.*, 2006; Woods *et al.*, 2012, 2013].
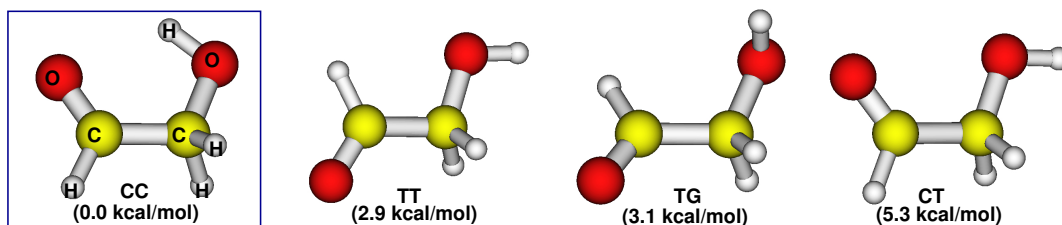

Figure 5.1. : The four stable conformers of GA: CC, TT, TG, and CT. Energies are relative to the CC conformer without zero point energy corrections, calculated at B3LYP/6-31+G* level of theory.

Glycolaldehyde (GA) is the simplest possible sugar which is also known as diose. GA molecule has four conformers (see Figure 5.1) viz., CC, TT, TG, and CT (C, T, and G, respectively, refer to cis-, trans-, and gauche conformations around the C-C and C-O bonds) [Senent, 2004]. Among its four conformers, the CC form is the most stable due to an intramolecular H-bond [Senent, 2004] and is the only conformer detected in the interstellar clouds [Hollis *et al.*, 2001]. GA has been detected in the atmosphere as a product of photochemical oxidation of volatile organic molecules such as ethene and isoprene [Magneron *et al.*, 2002; Zhou *et al.*, 2009; Yokelson *et al.*, 1997] in addition to direct emission from biomass burning [Niki *et al.*, 1987; Bacher *et al.*, 2001]. Decay of GA in the troposphere occurs mainly via OH radical reaction and photochemical decomposition. Photolysis reaction of GA has been investigated in solution [Beeby *et al.*, 1987] and in the gas phase [Zhu and Zhu, 2010; Chin *et al.*, 2014]. Porterfield et al. [Porterfield *et al.*, 2016], have studied the pyrolysis of GA and products such as H, CO, HCHO, CH$_2$CO, etc. were identified

using photo-ionization mass spectrometry. More than two hundred organic molecules have been detected in the interstellar medium and GA is the only sugar among them [Hollis *et al.*, 2000, 2004; Beltrán *et al.*, 2008; Li *et al.*, 2017; De Simone *et al.*, 2017]. GA combines with propenal resulting in ribose, a central component of RNA, and hence GA is considered to be a precursor of RNA [Sharma *et al.*, 2016]. Even though GA has been detected in space, no well established mechanism for the gas phase formation of GA is available in the literature. For instance, formation of protonated GA from association reaction between formaldehyde and protonated formaldehyde in the interstellar medium was considered [Halfen *et al.*, 2006] but later this reaction was shown to be inefficient [Woods *et al.*, 2012, 2013].

Relevant to the formose reaction, gas phase fragmentation of deprotonated GA, $C_2H_3O_2^-$ was investigated by Uggerud and co-workers [Sekiguchi and Uggerud, 2013]. From a retro-synthetic point of view, dissociation of the conjugate base of GA forming $HCO^- + HCHO$ products was investigated using tandem mass spectrometry under collision induced dissociation (CID) conditions [Papayannopoulos, 1995]. Experiments were carried out for a range of collision energies (0.2 - 20 eV) and the $HCO^- + HCHO$ products were not identified as primary decomposition products of deprotonated GA. Signal at m/z = 31, corresponding to the reaction $C_2H_3O_2^- \longrightarrow CO + CH_3O^-$, was the dominant peak in the mass spectrum. Other than this work, there are no studies in the literature reporting the fragmentation chemistry of the deprotonated GA. In the present work, dissociation chemistry of deprotonated GA was investigated using detailed electronic structure theory calculations and classical direct chemical dynamics simulations[Sun and Hase, 2003; Paranjothy *et al.*, 2013] to model the collision induced dissociation experiments by Uggerud and co-workers [Sekiguchi and Uggerud, 2013]. The trajectory initial conditions were selected to mimic single collision conditions in the gas phase. A variety of decomposition products including $HCO^- + HCHO$ were identified. Simulation results were compared with previously reported CID experiments and detailed atomic level dissociation mechanisms are presented.

5.1 COMPUTATIONAL METHODOLOGY

Electronic structure calculations and the direct classical trajectory integrations were performed using the density functional B3LYP method utilizing the 6-31+G* basis set and the limited computational costs associated with the method. A comparison of stationary point energies computed using B3LYP/6-31+G* method and higher level methods is presented in the Table 5.1. Deprotonation of GA (CH$_2$OHCHO) can occur at three positions viz., carbonyl carbon (CH$_2$OHCO, 1X), the second carbon atom (CHOHCHO, 1C), and the hydroxyl group (CH$_2$OCHO, 1O). Geometries of these species were optimized using the B3LYP/6-31+G* method and the results are shown in Figure 5.2. 1C is the lowest energy isomer (0.0 kcal/mol) followed by 1O (4.0 kcal/mol) and 1X (21.6 kcal/mol).
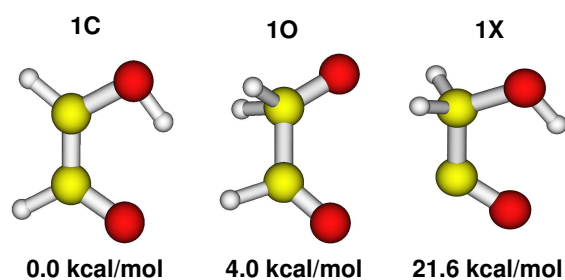

Figure 5.2. : Optimized geometries and relative energies of deprotonated glycolaldehyde. Energies are relative to the lowest energy 1C isomer without zero point energy corrections.

Potential energy profiles of possible dissociation pathways (based on previous work [Sekiguchi and Uggerud, 2013]) of deprotonated GA were characterized using B3LYP/6-31+G* method. All the stationary points were geometry optimized and normal mode frequency calculations were performed to differentiate an equilibrium point from a transition state. Intrinsic reaction coordinate (IRC) calculations were performed to ascertain whether a given transition state connects correct product(s) with the reactant. The results are summarized in Figure 5.3 wherein the given energies (in kcal/mol) are relative to 1C without zero point energy corrections. The reaction of interest (deprotonated GA $\longrightarrow HCO^- + HCHO$) occurs from the 1O isomer and a direct reaction path from the lowest energy 1C isomer does not exist. The reaction is exoergic by 52.2 kcal/mol with respect to 1O and the energy profile does not have a saddle point. Intramolecular hydrogen transfer resulting in 1O from 1C has a barrier of 46.2 kcal/mol and the torsional rotation of $C-C$ resulting in the geometrical isomer 1T requires energy of 43.0 kcal/mol. Dissociation of 1O forming $CH_3O^- + CO$ and dehydrogenation of 1C leading to $HCO^- + CO + H_2$ products are also shown in Figure 5.3. Transition state for the $CH_3O^- + CO$ product formation has an energy of 32.1 kcal/mol with respect to 1O. The $HCO^- + CO + H_2$ products have high energy in comparison to $HCO^- + HCHO$ and $CH_3O^- + CO$ products. Optimized geometries of various stationary points on the dissociation energy profile of deprotonated GA are provided in the Figure 5.4. Detailed descriptions of the various stationary points of deprotonated glycolaldehyde used in Figure 5.4, are described below.

Table 5.1. : Stationary point energies of dissociation of deprotonated GA computed using different methods. Energies are in kcal/mol, relative to 1C without zero point energy corrections.

species[a]	B3LYP 6-31+G*[b]	MP2/ 6-31+G*	CCSD(T)/ 6-31+G*[c]	MP2/ 6-311++G**	CCSD(T)/ 6-311++G**[d]
1C	0.0	0.0	0.0	0.0	0.0
TS$-$1O	46.4	48.3	50.0	49.3	50.4
1O	6.8	6.6	5.9	9.1	8.0
TS$-$CO	38.8	45.1	40.1	46.2	40.8
CO$-$H$_3$CO	22.6	19.6	17.6	20.6	17.9
H$_3$CO$^-$ + CO	27.9	22.2	20.5	23.3	20.9
HCO$^-$ + H$_2$CO	58.3	60.4	55.8	61.9	56.7
TS$-$1T	43.1	43.9	41.1	42.6	39.7
1T	7.8	9.1	8.4	8.5	7.9
TS$-$H$_2$	48.0	53.9	54.3	51.3	51.4
H$_2$$-$CHOCO	35.4	35.2	32.2	39.2	36.6
CHOCO$^-$ + H$_2$	37.6	37.1	33.9	41.7	38.9
HCO$^-$ + H$_2$ + CO	68.0	63.2	57.5	64.3	58.4

[a]description of various stationary points such as TS-1O, etc. is given below
[b]theory used in dynamics simulations
[c]single point energies computed using geometries optimized at the MP2/6-31+G* theory
[d]single point energies computed using geometries optimized at the MP2/6-311++G** theory

- CHOCH$_2$OH $\xrightarrow{-H}$ 1C

    – 1C represents deprotonation on methylene carbon of glycolaldehyde i.e. (CHOC̄HOH).

- CHOCH$_2$OH $\xrightarrow{-H}$ 1O

    – 1O represents deprotonation on hydroxide group of glycolaldehyde i.e. (CHOCH$_2$O$^-$).

- CHOCH$_2$OH $\xrightarrow{-H}$ 1X

- – 1X represents deprotonation on aldehyde carbon of glycolaldehyde i.e. ($^-$COCH$_2$O).

- 1C → TS-1T → 1T → TS-H$_2$ → H$_2$-CHOCO → H$_2$ + CHOCO$^-$ → H$_2$ + CO + HCO$^-$

  - – TS-1T is the transition state connecting 1C with 1T, where 1T represents geometric isomer resulting from C-C bond rotation of 1C.

  - – TS-H$_2$ is the transition state connecting 1T with H$_2$-CHOCO complex.

- 1C → TS-1O → 1O → TS-CO → CO-H$_3$CO → CO + H$_3$CO$^-$

  - – TS-1O is the transition state connecting 1C with 1O.

  - – TS-CO is the transition state connecting 1O with CO-H$_3$CO complex.

- 1C → TS-H$_2$O → H$_2$O + HCCO$^-$

  - – TS-H$_2$O is the transition state connecting 1C with H$_2$O + HCCO$^-$.

- 1C → TS-CH$_2$CO → CH$_2$CO + OH$^-$

  - – TS-CH$_2$CO is the transition state connecting 1C with CH$_2$CO + OH$^-$.

- 1O → TS$-$1,2H$-$1O → 1O

  - – TS$-$1,2H$-$1O is the transition state for 1,2 H-transfer in 1O.

- 1C → TS$-$1,4H$-$1C → 1C

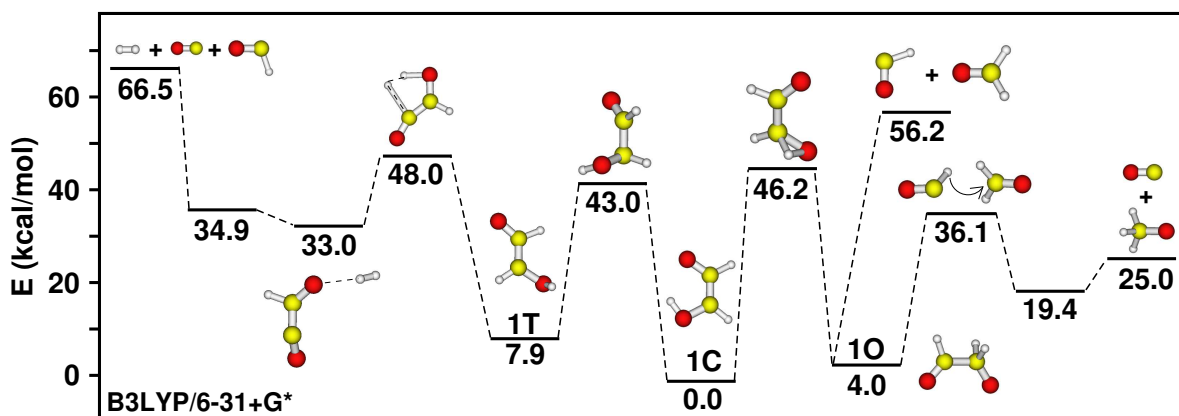 - – TS$-$1,4H$-$1C is the transition state for 1,4 H-transfer in 1C.

Figure 5.3. : Potential energy profiles of dissociation of deprotonated GA computed using B3LYP/6-31+G* level of electronic structure theory. The given energies (in kcal/mol) are relative to that of 1C and zero point energy not corrected.

Collision induced dissociation experiments of deprotonated GA were modeled using Born-Oppenheimer direct chemical dynamics simulations [Sun and Hase, 2003; Paranjothy *et al.*, 2013] to establish atomic level reaction mechanisms. Classical trajectories were initiated from 1C and 1O isomers and they were excited by collision with an Ar atom. Vibrational and

Table 5.2. : Fractions of Trajectories Showing Various Pathways Following Collisional Activation of deprotonated GA.

pathway	1C				1O			
	2 eV	5 eV	9 eV	13eV	2 eV	5 eV	9eV	13eV
$HCHO+HCO^-$ (m/z=29)	0	0	1	1	0	53	77	77
$HCHO+CO+H^-$ (m/z= 1)	0	0	2	2	0	0	10	16
$CO+H_2+HCO^-$ (m/z=29)	0	0	1	3	0	0	1	3
$H_2O+O=C=CH^-$ (m/z=41)	0	0	15	29	0	0	0	0
$CH_2=C=O+OH^-$ (m/z=17)	0	0	12	37	0	0	0	1
$CH_2+CO+OH^-$ (m/z=17)	0	0	0	3	0	0	0	0
$GA \longleftrightarrow GA$ (m/z=59) (hydride transfer)	40	65	37	17	19	21	5	0
$2CO+H_2+H^-$ (m/z= 1)	0	0	0	2	0	0	1	0
$CO+{}^-CH_2OH$ (m/z=31)	0	0	0	3	0	0	0	0
$CO+CH_3O^-$ (m/z=31)	0	0	0	0	0	4	3	2
$(CHO)_2+H^-$ (m/z= 1)	0	0	2	1	0	0	2	0
$2CHO+H^-$ (m/z= 1)	0	0	0	0	0	0	0	1
no reaction	60	35	30	2	81	22	1	0
total	100	100	100	100	100	100	100	100

rotational energies of the reactant species were selected from 300 and 75 K Boltzmann distributions, respectively, using standard algorithms [Peslherbe *et al.*, 1999; Papayannopoulos, 1995]. An initial separation of 10.0 Å was kept between the reactant molecule and the Ar atom and the collision occurred with an impact parameter of 0.0 Å. Reactant molecule was rotated randomly in each trajectory allowing for collisions at different sites of the molecule. Relative translational energy E_{rel} between the center-of-mass of the reactant molecule and the colliding Ar atom was fixed at four different values viz., 2, 5, 9, and 13 eV. These E_{rel} values were selected based on experiments [Sekiguchi and Uggerud, 2013]. Trajectories were integrated till 3 ps or until reaction products were separated by a distance of 12.0 Å using a 6th order Symplectic integrator [Schlier and Seiter, 1998, 2000] with a step-size of 0.5 fs. These simulation conditions were sufficient enough to maintain a good energy conservation in the trajectories. Total energy E_{tot} in the trajectories were approximately 75, 148, 240, and 330 kcal/mol at E_{rel} = 2, 5, 9, and 13 eV, respectively, for the selected initial conditions.

5.2 RESULTS AND DISCUSSION

Direct dynamics simulations were performed at four different relative collision energies starting from two different isomers of deprotonated GA. For each simulation, 100 trajectories were generated which amounts to a total of 800 direct dynamics trajectories. Total energy in the trajectories was conserved within $E_{tot} \pm 1.0$ kcal/mol. Trajectories were analyzed for establishing reaction pathways and mechanisms. A variety of reaction products were observed and a summary of trajectory events is given in Table 5.2 and the fractions of trajectories (n_T) branching into multiple reaction pathways are given in Figure 5.5. For both the 1C and 1O isomers, the reactivity increased with increasing collision energy.
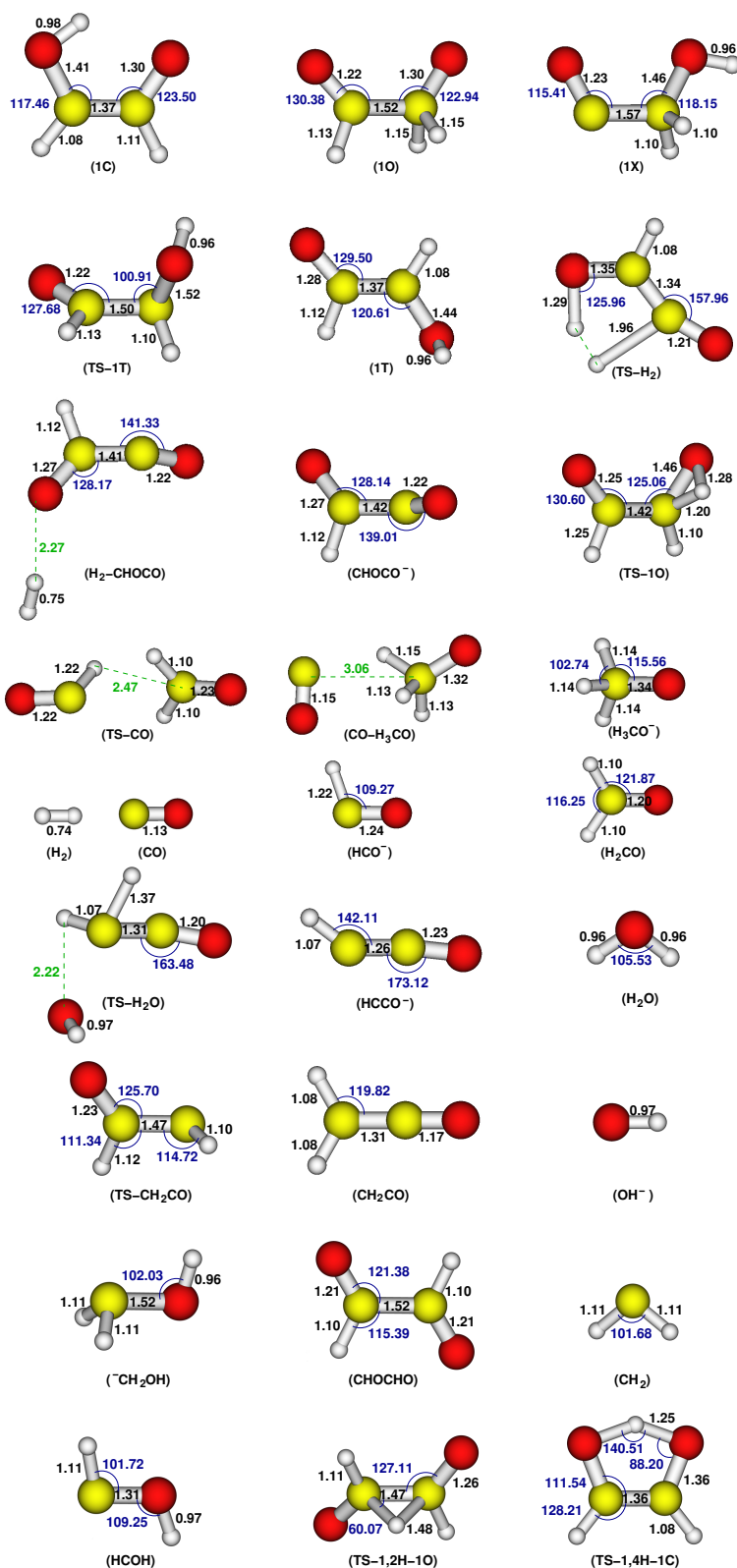
Figure 5.4. : Equilibrium geometries of deprotonated glycolaldehyde stationary points computed using B3LYP/6-31+G* theory.
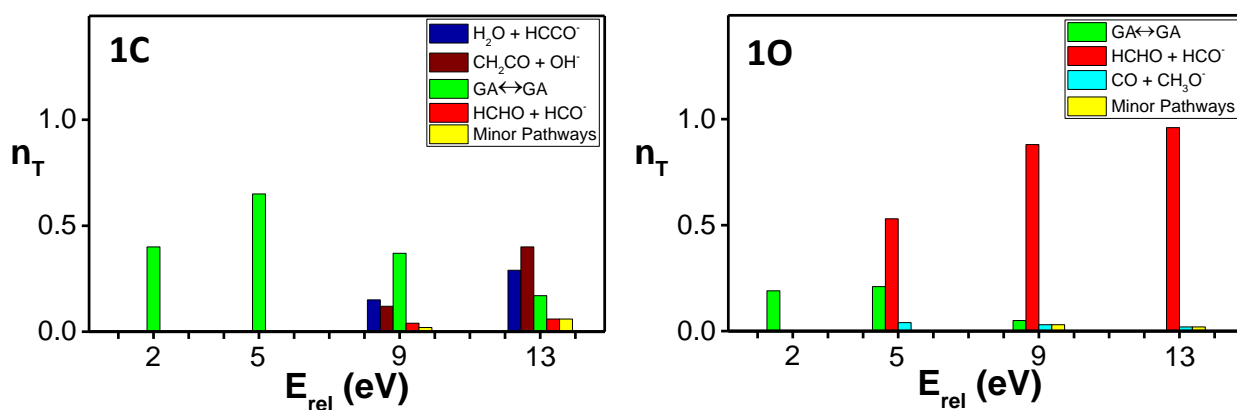
Figure 5.5. : Fractions of trajectories branching into multiple reaction pathways given as a function of E_{rel}.

5.2.1 Dynamics of 1C

As shown in Table 5.2, reactivity (defined as the dissociation or isomerization following collision with Ar atom before the trajectory stopping criterion was reached) for the 1C isomer was observed in 40, 65, 70, and 98 trajectories at E_{rel} = 2, 5, 9, and 13 eV, respectively. Primary dissociation of 1C observed in the simulations was that of C−O bond (involving O of the hydroxyl group, see Figure 5.2) resulting in the products OH^- (m/z=17) + CH_2CO or $H_2O + HCCO^-$ (m/z=41) (shown in Figure 5.6). In these reactions, the C−O bond dissociation is associated with intramolecular hydrogen (hydride) transfer. Electronic structure calculations at the B3LYP/6-31+G* level of theory were performed to characterize these reaction pathways and the results are shown in Figure 5.8(a) and (b). The H_2O elimination channel is endoergic (by 19.5 kcal/mol) and the reaction pathway has a transition state with energy of 69.8 kcal/mol relative to 1C. At E_{rel} = 9 and 13 eV, 15 and 29 trajectories, respectively, showed dissociation via this pathway. The ketene channel ($CH_2CO + OH^-$) has a reaction energy of 40.8 kcal/mol. Attempts to find a
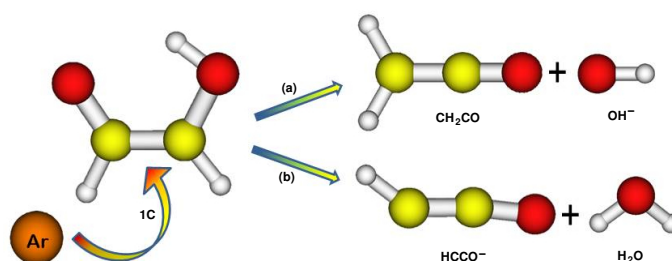

Figure 5.6. : Schematic representation of formation of (a) CH_2CO + OH^- and (b) $HCCO^-$ + H_2O from 1C isomer.

transition state for this pathway were unsuccessful. A total of 12 (9 eV) and 40 (13 eV) trajectories followed the ketene channel. Ketene has been observed in the flash pyrolysis of glycolaldehyde molecule [Porterfield *et al.*, 2016]. In a small number of trajectories (3 out of 40, 13 eV), ketene underwent subsequent dissociation resulting in $CH_2 + CO$. Ground state dissociation of ketene is known to be barrier-less and endoergic [Klippenstein *et al.*, 1996]. An important observation here is that the above mentioned two reactions occurred primarily via shattering [Martin Somer *et al.*, 2019] i.e., reaction occurred upon collision or within a very short time following the collision.
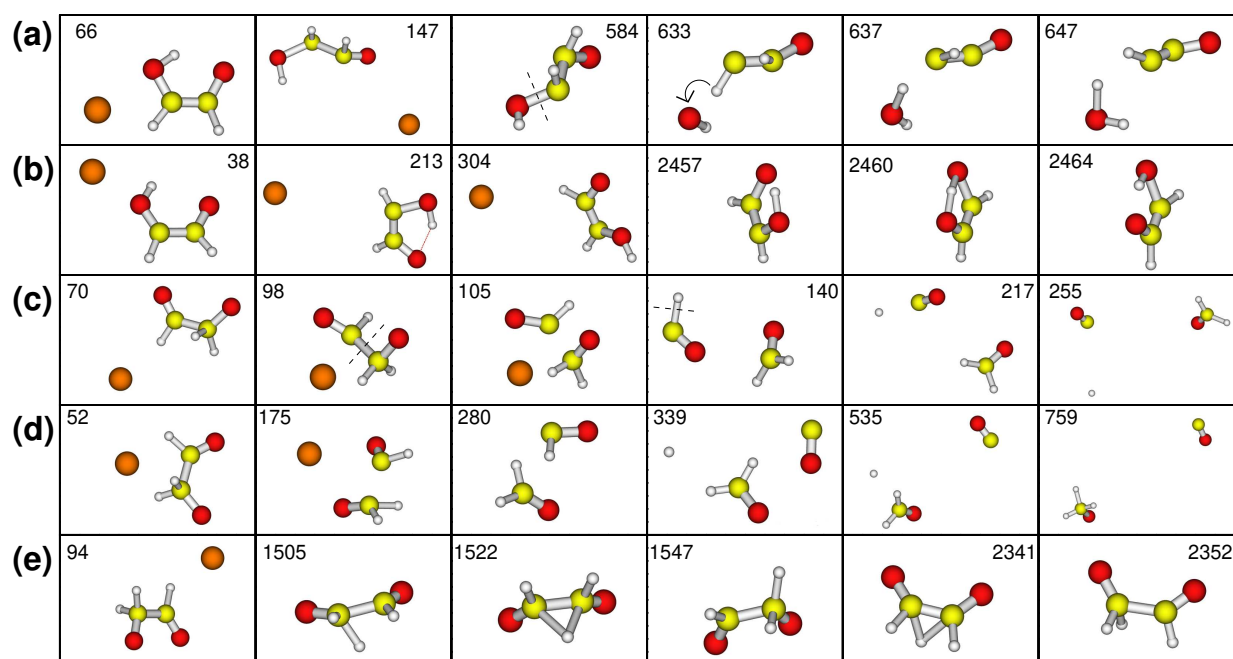
Figure 5.7. : Snapshots of example trajectories showing the reaction (a) $1C \longrightarrow H_2O + HCCO^-$, (b) $1C \longleftrightarrow 1C$, (c) $1O \longrightarrow HCO^- + HCHO \longrightarrow H^- + CO + HCHO$, (d) $1O \longrightarrow HCO^- + HCHO \longrightarrow CO + CH_3O^-$, and (e) $1O \longleftrightarrow 1O$. Numbers inside each frame is time in fs at which the snapshot was taken.

In a shattering mechanism, the molecule does not have enough time for the excitation energy to randomize among the modes of the molecule and this is a non-statistical reaction pathway [Martin Somer *et al.*, 2019]. Shattering mechanism has been identified in the collision induced dissociation of CH_3SH^+, $CH_3SCH_3^+$, and $Cr^+(CO)_6$ molecules [Martínez-Núñez *et al.*, 2004; Chen *et al.*, 2002; Martínez-Núñez *et al.*, 2006, 2005]. For the H_2O elimination pathway, the collision directly pushes the 1C molecule into the transition state configuration. Only in a very small number of trajectories, a finite time gap was observed between collision and the reaction. Previous studies [Martin Somer *et al.*, 2019] have shown that the shattering fragmentations can be overestimated in simulations in comparison to non-shattering mechanisms.

In a large fraction of the trajectories, intramolecular hydrogen transfer between the two O atoms was observed. This fraction is largest in the 5 eV simulation. The barrier for this reaction is 9.6 kcal/mol and the energy profile is shown in Figure 5.8(c). In some of the dissociating trajectories discussed above, intramolecular hydrogen transfer occurred prior to dissociation. The primary reaction of interest (GA $\longrightarrow HCHO + HCO^-$) was observed in negligible number of trajectories in these simulations. As can be seen from Figure 5.3, there is no direct reaction path from 1C to $HCHO + HCO^-$. In these trajectories, C−C dissociation of 1C occurred resulting in $HCOH + HCO^-$. The HCOH carbene, upon formation, immediately isomerized to HCHO or dissociated to $H_2 + CO$ products. In the 9 and 13 eV simulations, 4 and 6 trajectories, respectively, resulted in $HCHO + HCO^-$, however, HCO^- further dissociated to $H^- + CO$ products in some of these trajectories. Similarly, the formation of $CO + CH_3O^-$ (m/z=31) products was not observed in the simulations. However, in the 13 eV simulation, 3 trajectories showed formation of $CO + ^-CH_2OH$ (m/z=31) products. The $^-CH_2OH$ is a higher energy isomer (by 36.7 kcal/mol) of CH_3O^- and resulted via C−C dissociation of 1C with concomitant hydrogen transfer. In a large
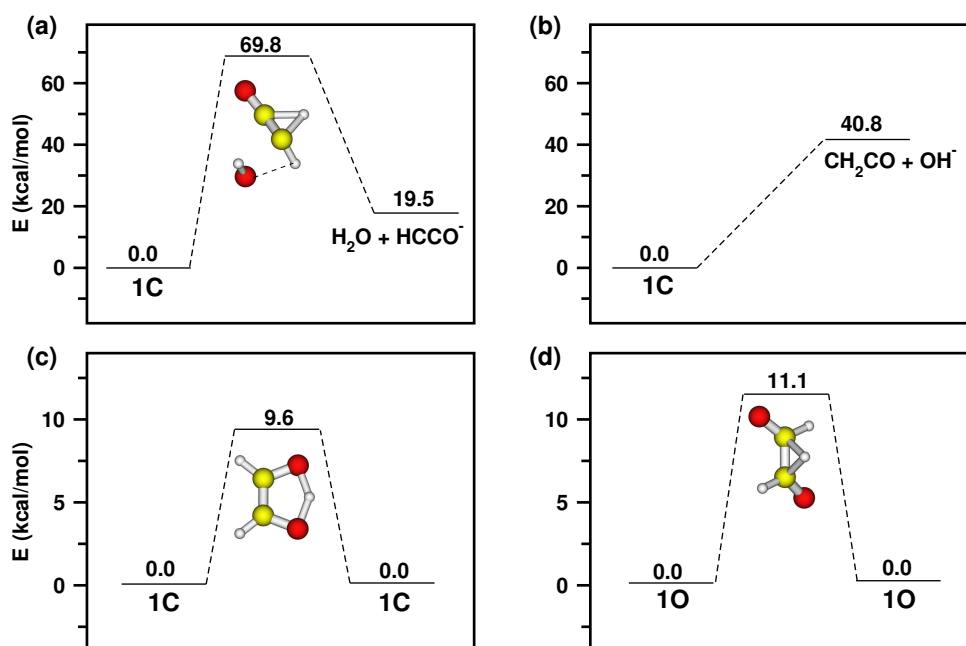
Figure 5.8. : Potential energy profiles for the reactions: (a) $1C \longrightarrow H_2O + HCCO^-$, (b) $1C \longrightarrow CH_2CO + OH^-$, (c) intramolecular hydrogen transfer in $1C$ and (d) $1O$. Energies are given in kcal/mol and are zero point energy not corrected.

fraction of trajectories in the low energy simulations, dissociation or isomerization of 1C was not observed. Snapshots of example trajectories showing these different reaction pathways are shown in Figure 5.7. Numbers inside each frame is time in fs at which the snapshot was taken. Formation of $H_2O + HCCO^-$ products can be seen in 5.7(a) wherein C−O dissociation and hydrogen transfer can be observed in the 584 and 633 fs frames, respectively. 5.7(b) shows an example intramolecular hydrogen transfer trajectory wherein the hydrogen shifts can be seen in the 213 and 2460 fs frames.
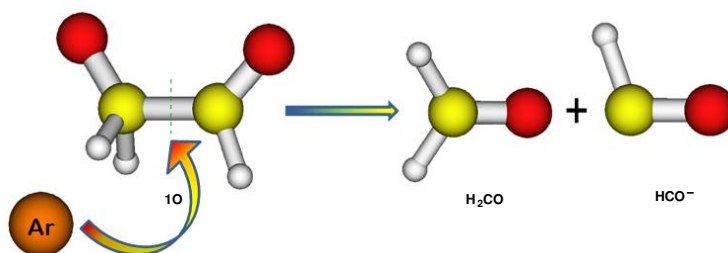
5.2.2 Dynamics of 1O

Figure 5.9. : Schematic representation of formation of reverse formose products from 1O isomer.

Dissociation dynamics of the slightly higher energy 1O isomer was quite different from that of 1C discussed above. The retro-formose reaction, resulting in the $HCO^- + HCHO$ products (Figure 5.9), was observed in these simulations in large fraction of trajectories. At E_{rel} = 2, 5, 9, and 13 eV, we observed 0, 53, 88, and 96 trajectories, respectively. This is a direct dissociation process with a reaction endoergicity of 56.2 kcal/mol (see Figure 5.3) and the search for a dissociation transition state was unsuccessful. Visualization of the trajectories showed that the $HCO^- + HCHO$

product formation from 1O occurs mainly via shattering mechanism [Martin Somer *et al.*, 2019] i.e., C−C dissociation occurs within a very short time after the collision with the Ar atom. Non-shattering type $1O \longrightarrow HCO^- + HCHO$ reaction i.e., longer time gaps between collision and dissociation occurred only in a very small number of trajectories in the low energy simulations. Note that for the 1C isomer also, major reaction paths (H_2O elimination and the ketene channel) followed a shattering type mechanism. Subsequent dissociation of $HCO^- + HCHO$ products was also observed in the high energy trajectories. Dissociation of HCO^- to $CO + H^-$ occurred in 10 and 16 trajectories, at E_{rel} = 9 and 13 eV, respectively. Also, dissociation of HCHO to $H_2 + CO$ occurred in a few trajectories in the high energy simulations (Table 5.2). Snapshots of an example trajectory forming $HCO^- + HCHO$ products are presented in Figure 5.7(c). The C−C dissociation and the subsequent reaction of HCO^- forming $H^- + CO$ can be observed in the 98 and 140 fs frames, respectively.

Experiments by Uggerud and co-workers [Sekiguchi and Uggerud, 2013] showed that a strong component at m/z = 31, corresponding to CH_3O^- product, was present in the CID spectra of deprotonated GA. In the present simulations, the reaction $1O \longrightarrow CO + CH_3O^-$ was observed in a small number of trajectories at E_{rel}= 5, 9, and 13 eV. Previous studies [Sekiguchi and Uggerud, 2013] and the present electronic structure theory calculations (Figure 5.3) show that the $1O \longrightarrow CO + CH_3O^-$ reaction occurs via a TS involving C−C bond dissociation with concomitant H atom transfer. This TS has a barrier of 32.1 kcal/mol relative to 1O. Interestingly, the trajectories that formed the $CO + CH_3O^-$ products, though smaller in number, did not follow this pathway. They first underwent C−C dissociation resulting in $HCHO + HCO^-$ products and after a small time period, H^- transfer occurred from HCO^- to HCHO resulting in the final products. Snapshots of an example trajectory showing this pathway are given in Figure 5.7(d). In this trajectory, $HCO^- + HCHO$ formation occurs at 175 fs followed by HCO^- dissociation around 300 fs. The hydride ion moves around and attaches with HCHO forming CH_3O^-. Similar to 1C, intramolecular hydride transfer between the two C atoms of 1O was ubiquitous in the trajectories though the fractions were less in the latter in comparison to the former. Barrier for the hydrogen transfer is 11.1 kcal/mol relative to 1O computed using B3LYP/6-31+G* level of theory and the energy profile is shown in Figure 5.8(d). Maximum number of trajectories showing this isomerization reaction was observed at E_{rel} = 5 eV. Snapshots of an example trajectory showing intramolecular hydrogen transfer is shown in Figure 5.7(e). The hydrogen atom transfers can be observed in the 1522 and 2341 fs frames. The H_2O elimination channel and the ketene channel were observed in an appreciable fraction of trajectories in the dissociation of the 1C isomer however these channels were not important for 1O as there are no direct reaction pathways.

5.3 DISCUSSION

CID experiments of deprotonated GA showed that the uncatalyzed, gas phase formose reaction $HCO^- + HCHO \longrightarrow HCOCH_2O^-$ is an unlikely event [Sekiguchi and Uggerud, 2013]. Electronic structure calculations show that the lowest energy isomer of deprotonated GA (1C) does not have a direct reaction pathway to form the retro-formose products. Consistently, direct dynamics simulations of 1C dissociation showed formation of $HCO^- + HCHO$ only in a small number of trajectories. On the other hand, the slightly higher energy 1O isomer resulted in the desired reaction products in a large number of trajectories. The reaction involves direct C−C dissociation without a transition state and requires energy of 52.2 kcal/mol relative to 1O. Unlike the uncatalyzed formose reaction, electronic structure theory studies have shown that metal ion catalyzed and hydrogen bond mediated dimerization of formaldehyde to form glycolaldehyde are nearly barrier-less processes [Thripati and Ramabhadran, 2017]. In an infrared spectroscopic photolysis study, Niki et al. [Niki *et al.*, 1987], found that OH radical primarily deprotonated GA from the carbonyl carbon and the other carbon atom to an yield of up to 80%. Deprotonation from

the hydroxyl group of GA results in 1O from which the retro-formose products $HCO^- + HCHO$ were mainly produced in the simulations. The 1O species formed only in least amounts in the experiments by Niki et al., and the branching ratios between these isomers were also confirmed in another study [Magneron *et al.*, 2005]. These observations indicate that the deprotonation of GA in the experiments by Uggerud and co-workers [Sekiguchi and Uggerud, 2013] may have primarily resulted in the 1C isomer and the formation of $HCO^- + HCHO$ products required further isomerization from 1C $\longrightarrow$ 1O and this reaction has a barrier of 46.2 kcal/mol. Lower 1O fractions observed in these experiments is probably why less retro-formose products were observed in the CID experiments by Uggerud and co-workers [Sekiguchi and Uggerud, 2013]. Another important observation in the present work is that the intramolecular hydrogen transfer was ubiquitous in the simulations. Energy barriers were of the order of 10 kcal/mol and was observed in appreciable number of trajectories especially in the 5 eV simulations. Intramolecular hydride shift has been invoked in the proposed mechanism of formose reaction in a recent experimental study [Appayee and Breslow, 2014].

As can be seen from Table 5.2, there are differences between the simulation results and CID experiments [Sekiguchi and Uggerud, 2013]. In particular, experiments showed larger peak intensity for the m/z = 31 signal in comparison to m/z = 29 signal. In the simulations, m/z = 31 species (CH_3O^- or $^-CH_2OH$) resulted in a smaller number of trajectories than m/z = 29 (HCO^-). This discrepancy may be rationalized as follows. Simulations showed that the $CH_3O^- + CO$ products formed via $HCO^- + HCHO$ products followed by intermolecular hydrogen transfer. In the simulations, a large fraction of trajectories resulted in $HCO^- + HCHO$ products but they separated immediately upon formation. In the experiments, multiple collisions and the proximity of the products ($HCO^- + HCHO$) in the collision cell might have led to the larger CH_3O^- fractions. To a small extent, m/z = 57 ion (dehydrogenation product) was detected in the experiments but was not observed in the simulations. Differences [Martin Somer *et al.*, 2019] in the abundance of product ions between experiments and chemical dynamics simulations can occur because simulations were performed under single collision conditions but the experiments might involve multiple collisions. Furthermore, shattering is typically overestimated in simulations and there are timescale differences between simulations (in ps) and experiments (upto ms).

5.4 SUMMARY

Classical chemical dynamics simulations modeling previously reported collision induced dissociation experimental study of deprotonated glycolaldehyde are reported in this chapter. The experimental study was performed to understand the gas phase reaction between formyl anion and formaldehyde in the interstellar media to form carbohydrates. The study concluded [Sekiguchi and Uggerud, 2013] that the efficiency for this reaction is low and the results of the present simulations are in qualitative agreement with this work. Deprotonation of GA can occur at three different sites and the dynamics simulations were performed for the lowest energy 1C isomer and slightly higher energy 1O isomer. The retro-formose reaction GA $\longrightarrow$ $HCHO + HCO^-$, occurred mainly from the slightly higher energy 1O isomer via a direct C−C dissociation. CID of the lowest energy 1C isomer resulted in the retro-formose products only in a very small number of trajectories. Analysis of the trajectories showed non-statistical nature of the dissociation dynamics of deprotonated glycolaldehyde.

...